Published in final edited form as:
J Immunol. 2011 August 1; 187(3): 1097–1105. doi:10.4049/jimmunol.1003496.

The PD-L1:B7-1 pathway restrains diabetogenic effector T cells *in vivo*

Alison M. Paterson[*], **Keturah E. Brown**[*], **Mary E. Keir**[*], **Vijay K. Vanguri**[†], **Leonardo V. Riella**[‡], **Anil Chandraker**[‡], **Mohamed H. Sayegh**[‡], **Bruce R. Blazar**[§], **Gordon J. Freeman**[¶], and **Arlene H. Sharpe**[*]

[*]Department of Pathology, Harvard Medical School, Boston, MA 02115

[†]Department of Pathology, University of Massachusetts Medical School, Worcester, MA 01655

[‡]Transplantation Research Center, Renal Division, Brigham & Women's Hospital, Children's Hospital, Harvard Medical School, Boston, MA 02115

[§]Masonic Cancer Center and the Department of Pediatrics, Division of Blood and Marrow Transplantation, University of Minnesota, Minneapolis, MN 55455

[¶]Department of Medical Oncology, Dana-Farber Cancer Institute, Department of Medicine, Harvard Medical School, Boston, MA 02115

Abstract

PD-L1 is a co-inhibitory molecule that negatively regulates multiple tolerance checkpoints. In the NOD mouse model PD-L1 regulates the development of diabetes. PD-L1 has two binding partners, PD-1 and B7-1, but the significance of the PD-L1:B7-1 interaction in regulating self-reactive T cell responses is not yet clear. To investigate this issue in NOD mice, we have compared the effects of two anti-PD-L1 antibodies that have different blocking activities. Anti-PD-L1 mAb 10F.2H11 sterically and functionally blocks only PD-L1:B7-1 interactions, while anti-PD-L1 mAb 10F.9G2 blocks both PD-L1:B7-1 and PD-L1:PD-1 interactions. Both antibodies had potent, yet distinct effects in accelerating diabetes in NOD mice: the 'single-blocker' 10F. 2H11 mAb was more effective at precipitating diabetes in older (13 week old) than in younger (6-7 week old) mice, while the 'dual-blocker' 10F.9G2 mAb rapidly induced diabetes in NOD mice of both ages. Similarly, 10F.2H11 accelerated diabetes in recipients of T cells from diabetic, but not prediabetic mice, while 10F.9G2 was effective in both settings. Both anti-PD-L1 mAbs precipitated diabetes in adoptive transfer models of $CD4^+$ and $CD8^+$ T cell-driven diabetes. Taken together, these data demonstrate that the PD-L1:B7-1 pathway inhibits potentially pathogenic self-reactive effector $CD4^+$ and $CD8^+$ T cell responses *in vivo*, and suggest that the immunoinhibitory functions of this pathway may be particularly important during the later phases of diabetogenesis.

Introduction

Programmed death-1 (PD-1; CD279) is an inhibitory receptor that attenuates TCR signaling by recruitment of phosphatases (1, 2). Interactions between PD-1 and its ligands PD-L1 (B7-H1; CD274) and PD-L2 (B7-DC; CD273) deliver inhibitory signals that regulate T cell activation, tolerance and immune-mediated tissue damage (3-8). PD-1:PD-L interactions regulate multiple tolerance checkpoints that prevent autoimmunity (3, 4). In addition, the PD-1:PD-L1 pathway plays a key role in controlling host defenses aimed at eradicating

Address correspondence to AHS (arlene_sharpe@hms.harvard.edu), Telephone: 617-432-6569; fax: 617-432-6570.

Disclosures: AHS and GJF have patents and receive patent royalties related to PD-1.

microbial pathogens and tumors (3, 9) and is an essential mediator of T cell exhaustion, contributing to lack of viral control during chronic infections as well as to T cell unresponsiveness in the suppressive tumor microenvironment (10, 11).

PD-L1 is constitutively expressed on mouse B cells, dendritic cells (DCs), macrophages, and T cells, and is further upregulated upon their activation (12). PD-L1 also is expressed on a variety of non-hematopoietic cell types, including vascular endothelial cells and pancreatic islet cells (3, 13, 14). The broad expression of PD-L1 on hematopoietic and nonhematopoietic cells suggests that PD-L1 may have important roles in inhibiting immune responses in both lymphoid and non-lymphoid organs. Our bone marrow chimera studies revealed that PD-L1 expression on non-hematopoetic cells can shield the pancreas from immune-mediated tissue damage in the NOD diabetes model (15).

We recently identified B7-1 (CD80), a ligand for CD28 and CTLA-4, as a second binding partner for PD-L1 in mice (16) and humans (17, 18). B7-1 associates with PD-L1 with an affinity of ~1.4 μM, two- to three-fold higher than that of B7-1 for CD28 and about one-third the affinity of PD-L1 for PD-1 (16). The interaction between B7-1 and PD-L1 bidirectionally inhibits T cell proliferation and cytokine production *in vitro* (16).

The individual contributions of PD-L1:B7-1 and PD-L1:PD-1 interactions in controlling T cell responses *in vivo* are not yet understood. Studies with PD-L1-deficient mice cannot distinguish between the absence of PD-L1:B7-1 or PD-L1:PD-1 interactions. In addition, we have found that most commonly used anti-PD-L1 monoclonal antibodies (mAbs) block the interactions of PD-L1 with both PD-1 and B7-1. Thus, it is unclear whether functions previously attributed to PD-1:PD-L1 interactions are in fact due to B7-1:PD-L1 interactions, at least in part. Using an avidity-based adhesion assay, we characterized a panel of anti-mouse PD-L1 mAbs and identified a 'dual-blocker' mAb (that prevents binding of PD-L1 to PD-1 and B7-1) and a 'single-blocker' mAb (that prevents binding of PD-L1 to B7-1 only) – 10F.9G2 and 10F.2H11, respectively. Here we use the different blocking properties of these mAbs to compare the functional effects of both PD-L1 pathways *in vivo*, and elucidate a function for the novel PD-L1:B7-1 pathway.

We have chosen to compare the consequences of administering these two types of anti-PD-L1 mAbs to NOD mice, since we and others have demonstrated a critical role for PD-L1 in controlling self reactive T cell responses during NOD diabetes (14, 15). Blockade of PD-L1 with an anti-PD-L1 mAb (which is a dual-blocker) led to rapid onset of diabetes in one- and ten-week old prediabetic NOD mice (14). We found that PD-L1-deficient NOD mice develop markedly accelerated diabetes (15), and that PD-L1 can regulate the initial activation of potentially pathogenic T cells as well as the responses of pathogenic effector T cells (19, 20). Furthermore, diabetes is accelerated when either of the PD-L1 binding partners PD-1 or B7-1 is blocked or eliminated in NOD mice (14, 21, 22). Since PD-L1, PD-1 and B7-1 all have important roles in controlling NOD diabetes, the PD-L1:B7-1 pathway may regulate the initiation and/or progression of autoimmune diabetes. As PD-L1$^{-/-}$, PD-1$^{-/-}$ and B7-1$^{-/-}$ NOD mice all develop accelerated diabetes, it is challenging to use these mice as tools to dissect PD-L1:B7-1 versus PD-L1:PD-1 interactions *in vivo*. Here, we have compared the functional effects of anti-PDL1 mAbs that can block both PD-L1:B7-1 and PD-L1:PD-1 interactions (10F.9G2), or only PD-L1:B7-1 interactions (10F.2H11) during the development of NOD diabetes. Our studies show that B7-1:PD-L1 interactions, as well as PD-1:PD-L1 interactions, can restrain the responses of self-reactive T cells *in vivo*, and suggest that B7-1:PD-L1 interactions may be particularly important for regulating potentially pathogenic self-reactive effector T cells.

Materials and Methods

Mice

NOD/ShiltJ (NOD), NOD.CB17-Prkdc^{Scid}/J (NOD SCID) and NOD.Cg-Tg(TcraTcrbNY8.3)1Pesa/Dvs/J (8.3 NOD) mice were purchased from The Jackson Laboratory (Bar Harbor, ME). Additional 8.3 NOD mice were a gift from Mark Anderson. BDC2.5 NOD and Foxp3-GFP NOD mice were obtained from the JDRF Center on Immunological Tolerance in Type-1 Diabetes (Boston, MA) and bred to generate BDC2.5 Foxp3-GFP NOD mice. Transgenic mice that constitutively overexpress PD-1 on T cells (PD-1A) transgenic mice have been reported previously (23). Harvard Medical School is accredited by the American Association of Accreditation of Laboratory Animal Care (AAALAC). Mice were maintained and used according to institutional and National Institute of Health (NIH) guidelines in a specific pathogen-free barrier facility. Only female mice were used in these experiments. Mice were monitored for high urine glucose (Diastix; Bayer Corporation, Elkhart, IN). Positive glucosuria readings were confirmed by blood glucose measurement (Ascensia Contour; Bayer Corporation). Diabetes was confirmed by two consecutive blood glucose measurements of ≥ 250 mg/dL. Mice were sacrificed at the indicated time points or upon the second hyperglycemia reading.

For *ex vivo* analyses, pancreatic lymph nodes (PLN), spleen and pancreata were removed and single cell suspensions were prepared using a 70 μm cell strainer (BD Biosciences, San Jose, CA). Pancreata were treated with collagenase P (Sigma, St Louis, MO) prior to dissociation.

For histology, pancreata were fixed in 10% buffered formalin, dehydrated in graded alcohols and xylenes, embedded in paraffin, and stained with hematoxylin and eosin. Islets were scored, in a blinded fashion, as peri-insulitic if mononuclear cells were surrounding the islet, insulitic if mononuclear cells were invading the islets, or normal if no mononuclear cells were surrounding or within the islets. Slides with fewer than five islets were excluded from analysis. At least four slides, from individual mice, were analyzed per group.

Antibodies and flow cytometry

Anti-PD-L1 antibodies 10F.9G2 (24) and 10F.2H11 (16) (both Rat IgG2b) and Rat IgG2b isotype control antibody (clone LTF-2; BioXCell, West Lebanon, NH) were dialyzed against PBS, sterile filtered and tested for endotoxin (LAL assay) and found to have below 2 EU/mg. For *in vivo* antibody administration, mice were given 0.5 mg antibody on day 0, followed by 0.25 mg on days 2, 4, 6, 8 and 10 (all *i.p.*). If a mouse became diabetic before day 10, treatment was ceased.

For surface staining, 10F.9G2, 10F.2H11 and isotype control antibodies were directly conjugated to Alexa Fluor 488 using a protein labeling kit (Invitrogen, Eugene, OR) or were detected using goat anti-rat IgG (H+L) conjugated to Alexa Fluor 647 (Invitrogen). mAbs specific for CD3 (145-2C11), CD8 (53-6.7), CD4 (RM4-5), CD62L (MEL-14), CD44 (IM7), IFNγ (XMG1.2), TNFα (MP6-XT22) and PD-L1 (MIH5) were used for surface or intracellular staining (BioLegend, San Diego, CA). For cell surface stains, single cell suspensions were pre-incubated with purified anti-mouse CD16/32 Fc block (2 μg/ml; eBioscience, San Diego, CA) for 10 min, incubated for 30 min in 1-2 μg/ml of fluorochrome-conjugated antibody and then washed twice in 1% heat-inactivated fetal calf serum (FCS)/2 mM EDTA/PBS. For intracellular staining, cells were stimulated for 5 hr in 100 ng/ml phorbol myristate acetate (PMA) and 500 ng/ml ionomycin (both Sigma) in the presence of GolgiStop (BD Biosciences, San Jose, CA). Cells were then stained for surface markers as above and processed using a Cytofix/Cytoperm Fixation/Permeabilization Solution kit (BD Biosciences) according to the manufacturer's instructions. Positive gates

were defined using appropriate isotype control antibodies. For CFSE-dilution studies (see *In vitro T cell activation*), cells were stained with anti-CD4 and anti-CD8 and with 7-amino-actinomycin D (7-AAD; BioLegend) according to the manufacturer's instructions.

For cross-blocking studies, cells were incubated for 30 mins with purified 10F.9G2, 10F.2H11 or Rat IgG2b (20 μg/ml), washed and then stained with fluorescently-conjugated mAb using the above surface staining procedure. Cell analyses were performed using FACSCalibur or LSR II flow cytometers (BD Biosciences) and FlowJo software (Treestar, Ashland, OR).

In vitro T cell activation

Plates (96-well flat-bottom; BD Biosciences) were coated overnight at 4°C with 4 μg/ml anti-CD3 (clone 2C11; BD Biosciences) and 20 μg/ml mouse PD-L1-Human Fc IgG1 fusion protein (R&D Systems, Minneapolis, MN) or control Human Fc IgG1 (BioXCell) diluted in PBS. The next day, plates were washed three times with PBS and then incubated at 37°C for 3 hr with a range of concentrations of 10F.9G2, 10F.2H11 or Rat IgG2b isotype control Abs diluted in PBS. Plates were then washed three times with PBS and 1×10^5 T cells ($CD4^+$ and $CD8^+$) from PD-1A transgenic mice were added. $CD4^+$ and $CD8^+$ T cells were simultaneously isolated by positive selection using MACS (Miltenyi Biotec, Auburn, CA) beads and columns and labeled with Vybrant CFDA SE (CFSE) Cell Tracer Kit (Invitrogen). After 3 days, proliferation was assessed by flow cytometry and supernatants were harvested for IFNγ analysis.

Adoptive transfers

For adoptive transfers, NOD donors were confirmed to be euglycemic (~100 to 120 mg/dL) or diabetic (>250 mg/dL) by blood glucose measurement. Donor inguinal, brachial, axillary and pancreatic lymph nodes and spleens were isolated, pooled and subjected to the indicated cell isolation procedures. For adoptive transfer of total NOD T cells, $CD4^+$ and $CD8^+$ T cells were simultaneously isolated by positive selection using MACS beads and columns (Miltenyi Biotec, Auburn, CA). T cells ($9\text{-}10 \times 10^6$) from pre-diabetic or diabetic NOD donors were transferred by *i.v.* injection into NOD SCID recipients. For adoptive transfer of BDC2.5 T cells, $CD4^+$ T cells were isolated from BDC2.5 Foxp3-GFP NOD mice by MACS (Miltenyi Biotec) and sorted using a FACS Aria cell sorter (BD Biosciences), and 2×10^4 $CD4^+$Foxp3-GFP^- T cells were transferred *i.v.* into NOD SCID recipients. For adoptive transfer of 8.3 NOD T cells, $CD8^+$ T cells from 8.3 NOD mice were isolated by MACS, and $4 – 6 \times 10^6$ T cells were transferred *i.v.* into NOD SCID recipients. For all transfer experiments, T cell purity was assessed by flow cytometry and was consistently >96% after MACS isolation and >99% after sorting.

ELISA

For PD-L1 studies, Nunc ELISA-plates (Thermo Scientific, Roskilde, Denmark) were coated with anti-PD-L1 mAbs overnight in PBS. The following day, plates were blocked with 2% BSA/PBS for 1 hr at 37°C and then incubated with mouse PD-L1-Human Fc IgG1 fusion protein (R&D Systems) or control Human Fc IgG1 (BioXCell) at 1 μg/ml for 3 hr at 37°C. Plates were washed and incubated with biotinylated anti-human IgG (Jackson ImmunoResearch Laboratories, West Grove, PA) for 45 min at room temperature and then washed. For IFNγ assays, 4 μg/ml purified anti-IFNγ capture Ab (clone AN-18; eBioscience) and 1 μg/ml biotinylated anti-IFNγ detection Ab (clone XMG1.2; BD Biosciences) were used. Supernatants were compared against a standard curve of rIFNγ standard (Peprotech Inc., Rocky Hill, NJ). All ELISAs were incubated with HRP-conjugated Streptavidin (Pierce Endogen; Thermo Scientific) at 0.3 μg/ml for 30 min at room temperature, then developed using 3,3′,5,5′-Tetramethyl-benzidine liquid substrate system

(Sigma) and stopped using 0.5 M H_2SO_4. ELISAs were read at 450 nm on a SpectraMax 340PC plate reader and analyzed using Softmax Pro software, both from Molecular Devices (Sunnyvale, CA).

Statistics

p values were obtained using Prism software to calculate unpaired Student's t-tests or, for survival curves, Log-rank (Mantel-Cox) tests.

Results

10F.2H11 mAb sterically and functionally blocks only PD-L1:B7-1 interactions, while 10F.9G2 blocks both PD-L1:B7-1 and PD-L1:PD-1 interactions

We previously have described a pair of anti-PD-L1 mAbs that have distinct abilities to block the binding of PD-L1 to its two binding partners PD-1 and B7-1 (16). Based on an *in vitro* adhesion assay the 10F.9G2 mAb was found to be a 'dual-blocker', preventing binding of 300.19-PD-L1 transfectants to wells coated with PD-1- or B7-1-Ig fusion proteins. In contrast, the 10F.2H11 mAb blocked adhesion of PD-L1 transfectants to B7-1, but did not impair binding of PD-L1 transfectants to PD-1 fusion protein (16). To further characterize these two anti-PD-L1 mAbs, we first compared their affinities for binding to PD-L1 protein by ELISA, and determined that these two anti-PD-L1 mAbs have comparable affinities for PD-L1 (Fig. 1A). When used at the same concentration, 10F.9G2 and 10F.2H11 also similarly stained PD-L1-transfected 300.19 cells (Fig. 1B).

We next investigated whether PD-L1 could functionally engage PD-1 when bound by the 10F.2H11 mAb. Despite its inability to block PD-L1:PD-1 binding in adhesion assays, it was possible that 10F.2H11 could bind to PD-L1 in a manner that hindered functional PD-L1:PD-1 interactions. We assessed PD-1 engagement using an *in vitro* assay with T cells from transgenic mice (PD-1A) that constitutively over-express PD-1 on T cells (23). In previous studies we have shown that co-crosslinking of CD3 and PD-1 on PD-1A T cells, can inhibit anti-CD3-driven proliferation. We modified this assay and preincubated plate-bound PD-L1 with 10F.9G2 or 10F.2H11 prior to addition of PD-1A T cells. We found that 10F.9G2, but not 10F.2H11, could rescue inhibition of T cell proliferation (Fig. 1C). Likewise, 10F.9G2, but not 10F.2H11, rescued the inhibition of IFNγ production in these assays (Supplemental Fig. 1). Thus, the binding of 10F.2H11 to PD-L1 does not prevent the functional engagement of PD-1 by PD-L1. Therefore, 10F.2H11 can serve as a novel tool to interrogate the function of PD-L1:B7-1 interactions *in vivo* because it does not disrupt PD-L1:PD-1 and solely affects PD-L1:B7-1 interactions.

We also assessed whether 10F.9G2 and 10F.2H11 bound to overlapping epitopes on PD-L1. 300.19-PD-L1 transfectants were pre-incubated with saturating concentrations of purified 10F.9G2, 10F.2H11 or rat IgG2b isotype control mAb and then stained with fluorescently labeled 10F.9G2 or 10F.2H11 mAb. 10F.2H11 mAb was not able to block 10F.9G2 binding to PD-L1 and *vice versa* (Fig. 2A), suggesting that the 10F.2H11 and 10F.9G2 recognize distinct epitopes on PD-L1. We also compared the abilities of 10F.9G2 and 10F.2H11 mAbs to block the binding of a third anti-PD-L1 mAb, clone MIH5, which, like 9G2 is a dual blocker of PD-L1:PD-1 and PD-L1:B7-1 (unpublished observation). 300.19-PD-L1 transfectants were pre-incubated with saturating concentrations of purified 10F.9G2, 10F.2H11 or Rat IgG2b isotype control and then stained with fluorescently conjugated MIH5 antibody. While pre-incubation with 10F.2H11 mAb had no effect on MIH5 binding, 10F.9G2 pre-incubation dramatically reduced the level of MIH5 binding (Fig. 2B), suggesting that the 10F.9G2 and MIH5 dual blockers bind to overlapping epitopes that are distinct from the epitope recognized by 10F.2H11. We obtained similar data when cells from 10F.9G2- or

10F.2H11-treated mice were stained with MIH5 (data not shown). Our understanding of the binding activities of these two anti-PD-L1 mAbs is depicted in Fig. 2C.

10F.2H11 precipitates diabetes in NOD females in an age-dependent manner

We chose to examine the functional significance of PD-L1:B7-1 interactions in the NOD model of autoimmune diabetes because we and others have identified a key role for PD-L1 during the initiation and progression of NOD diabetes (14, 15). In the NOD mouse, disease develops through characteristic stages that begin with peri-insulitis (~3 to 4 weeks of age) and progress to insulitis (~8 to 10 weeks of age). Onset of diabetes occurs in a small percentage of females at ~12-13 weeks of age, with incidence approaching 90-100% by 30 weeks of age. Since PD-L1 can regulate both the initial activation of potentially pathogenic self-reactive T cells, as well as the responses of pathogenic self-reactive effector T cells in NOD mice, we compared the effect of PD-L1 blockade by administration of 10F.2H11 and 10F.9G2 anti-PD-L1 mAbs to female NOD mice of different ages. We gave the anti-PD-L1 mAbs to non-diabetic 6-7 or 13 week-old NOD mice in order to compare the effects of these anti-PD-L1 mAbs at early and late phases during the evolution of diabetes. When given to either 6-7 or 13 week-old NOD mice, the 10F.9G2 mAb had profound effects, resulting in diabetes in 90% of the treated mice within 7 days (Fig. 3A and 3B). In contrast, the 10F. 2H11 mAb was significantly less effective than 10F.9G2 ($p=0.0016$) in precipitating diabetes in 6-7 week-old females, leading to diabetes in 40% of these mice over a 14 day period (Fig. 3A). However, 10F.2H11 was almost as effective as 10F.9G2 in precipitating diabetes in 13 week-old female mice (Fig. 3B), resulting in diabetes in 80% of these mice over a two-week period. These data demonstrate the PD-L1:B7-1 interaction can inhibit self-reactive T cell responses *in vivo.* The strong effect of blocking the PD-L1:B7-1 interaction in the older mice suggests that this pathway may be particularly important in restraining effector T cell responses.

We compared the histology of pancreata from 10F.9G2-, 10F.2H11- or isotype control-treated mice. Pancreata were harvested 2 days after the development of diabetes or, if the mice remained healthy, at 14 days. Pathologic alterations were consistent with clinical manifestations of disease (Supplemental Fig. 2A and 2B). In the 6-7 week old mice, insulitis was higher in 10F.9G2-treated as compared to the 10F.2H11-treated mice, but insulitis was comparable in the 10F.9G2- and 10F.2H11-treated 13-week old mice. To assess the effects of these two anti-PD-L1 mAbs on T cell infiltration into pancreatic islets at the time when these anti-PD-L1 mAbs have distinct effects, we administered these mAbs to 6 week-old NOD females for two days (days 0 and 2) and then harvested all mice on the following day for histologic evaluation. Pancreata from 10F.9G2-treated mice showed intense insulitis with dense inflammatory infiltrates (Fig. 3C). There also were marked infiltrates in pancreata of 10F.2H11-treated mice as compared to isotype control- treated mice, but insulitis was less severe compared to 10F.9G2-treated mice. Insulitis was present in almost 100% of the islets from 10F.9G2-treated mice as compared to 50% from 10F.2H11-treated mice. In isotype control-treated NOD mice few islets showed peri-insulitis (~6%) or insulitis (~3%). These findings further demonstrate that B7-1:PD-L1 interactions regulate the development of autoimmune diabetes, particularly the progression to insulitis.

T cells from diabetic mice are more susceptible to the effects of 10F.2H11 antibody than T cells from prediabetic mice

To investigate whether 10F.2H11 distinctly affects T cells at different stages of their activation, we used an adoptive transfer approach. We compared the effects of 10F.2H11 or 10F.9G2 mAb administration to NOD SCID recipients of T cells from either pre-diabetic or diabetic NOD donors. As expected, prediabetic mice had lower proportions of activated T cells than their diabetic counterparts, as defined by CD62L and CD44 surface expression

(data not shown). The 10F.9G2, but not the 10F.2H11 mAb, accelerated the onset of diabetes such that within 4 weeks after transfer, ~50% of recipients of T cells from non-diabetic donors developed diabetes (Fig. 4A). However, the 10F.9G2 and 10F.2H11 mAbs similarly accelerated the onset of diabetes in NOD SCID recipients of T cells from diabetic NOD donors (Fig. 4B). These findings further support a role for B7-1:PD-L1 interactions in preferentially regulating effector T cell responses. Histological analyses of pancreata from adoptive transfer recipients 10 days after adoptive transfer were consistent with these disease outcomes; insulitis was observed only in 10F.9G2-treated recipients of T cells from prediabetic NOD mice, but in both 10F.9G2- and 10F.2H11-treated recipients of T cells from diabetic mice (Fig. 4C and 4D). These histologic results suggest that B7-1:PD-L1 interactions influence late diabetes checkpoints. Taken together, these data further demonstrate a functional effect of the PD-L1:B7-1 interaction *in vivo*, and implicate this pathway in restraining effector T cell function as opposed to priming.

10F.2H11 mAb promotes diabetes following transfer of islet antigen-specific $CD4^+$ and $CD8^+$ effector T cells

We compared the effects of the 10F.9G2 and 10F.2H11 mAbs on diabetogenic $CD4^+$ T cell responses. Diabetes can be transferred to NOD mice by islet antigen-specific effector $CD4^+$ T cells independently from $CD8^+$ T cells. For these studies, we used $CD4^+$ T cells from BDC2.5 NOD mice, which have a TCR from a diabetogenic T cell clone specific for chromogranin A, a pancreatic β-cell antigen (25, 26). BDC2.5$^+$ T cells that have been sorted to remove regulatory T cells are able to transfer diabetes to NOD SCID recipients (27). To compare the effects of the 10F.2H11 and 10F.9G2 mAbs on $CD4^+$ T cell-driven diabetes, we transferred BDC2.5$^+$CD4$^+$Foxp3-GFP$^-$ T cells into NOD SCID recipients and gave them either 10F.9G2 or 10F.2H11 mAb. Both anti-PD-L1 mAbs similarly accelerated diabetes onset when compared to isotype control (Fig. 5A). These results indicate that B7-1:PD-L1 interactions limit $CD4^+$ T cell-mediated diabetogenesis.

We next examined the effects of 10F.9G2 and 10F.2H11 mAbs in a $CD8^+$ T cell-driven diabetes model. For these studies, we utilized the 8.3 NOD mouse which is a TCR transgenic mouse harboring $CD8^+$ T cells specific for a peptide derived from islet-specific glucose-6-phosphatase catalytic subunit related protein (IGRP) (28). Diabetes in 8.3 NOD mice is partially dependent on the presence of $CD4^+$ T cells, as Rag-2-deficient 8.3 NOD mice develop diabetes later and with lower incidence than Rag-2-sufficient 8.3 NOD mice, and this difference can be reversed by adoptive transfer of non-transgenic NOD $CD4^+$ T cells (28). Consistent with these results, we found that $CD8^+$ T cells from diabetic 8.3 NOD females were only able to transfer disease to NOD SCID recipients with low incidence and late onset (Fig. 5B). In marked contrast, administration of either 10F.9G2 or 10F.2H11 mAb to NOD SCID recipients of $CD8^+$ T cells from diabetic 8.3 NOD mice resulted in the rapid induction of diabetes in 100% of the recipient mice (Fig. 5B). By day 11 post transfer, mice were still normoglycemic (data not shown), but $CD8^+$ T cells had infiltrated into islets in 10F.9G2- and 10F.2H11-, but not isotype control-treated mice (Fig. 6A–D). Insulitis was seen in ~25% of islets from 10F.2H11-treated mice and ~40% from 10F.9G2-treated mice but less than 4% from isotype control treated mice.

To further assess the effects of the 10F.2H11 mAb on effector T cell responses in NOD SCID recipients of $CD8^+8.3^+$ T cells, we treated NOD SCID recipients of $CD8^+8.3^+$ T cells with either 10F.2H11 or isotype control mAbs every other day and analyzed them on days 3 and 11 post transfer. There were no differences in the numbers of cells undergoing cell death, as assessed by 7-AAD staining in splenocytes from isotype control- *vs.* 10F.2H11-treated mice (Supplemental Fig. 3A) and the numbers of transferred T cells and recipient dendritic cells were not decreased at any timepoint analyzed (Supplemental Fig. 3B). In fact, in anti-PD-L1-treated mice, $CD8^+$ T cells accumulated in the spleens of anti-PD-L1-treated

mice with the absolute number of $CD3^+CD8^+$ T cells from 10F.9G2- and 10F.2H11-treated mice being significantly elevated in comparison with isotype control-treated mice by day 11 post transfer (Fig. 7A). Both anti-PD-L1-treated groups displayed increased percentages of activated $CD8^+$ T cells in their spleens compared to isotype control, as defined by low surface expression of CD62L and high surface expression of CD44 (Fig. 7B). In addition, $CD8^+$ T cells within both anti-PD-L1 treated groups had higher percentages of $IFN\gamma^+TNF\alpha^+$ cells (Fig. 7C), and the production of these effector cytokines was higher on a per cell basis as indicated by the mean fluorescence intensity of intracellular stains (Supplemental Fig. 4).

We analyzed the expression of both PD-1 and B7-1 on donor 8.3^+ T cells following transfer into NOD SCID mice given isotype control-mAb, which were not expected to become diabetic. Expression of PD-1 and B7-1 on donor 8.3^+ T cells is low (1-2%) at the time of transfer and upregulation of these two PD-L1 receptors occurs within days of transfer, with B7-1 being more rapidly expressed. In the spleen, B7-1 is expressed on 22.2% ± 5 of transferred T cells by 3 days post-transfer, while only 4.4% ± 0.3 express PD-1 (Fig. 7D). The majority of 8.3^+ T cells in the spleen which express PD-1 co-express B7-1. PD-L1 is expressed on ~30% of donor T cells and remains at similar levels over the timeframe studied (data not shown). These findings indicate that PD-L1 could engage B7-1 and PD-1 on 8.3^+ T cells during the course of anti-PD-L1 mAb administration.

Taken together, our studies indicate that PD-L1:B7-1 interactions can inhibit self-reactive $CD8^+$ effector T cell responses *in vivo*, and suggest that PD-L1 may restrict "helpless" $CD8^+$ T cell responses (i.e. $CD8^+$ T cell responses generated in the absence of $CD4^+$ T cell help). Thus, using multiple approaches, we find that PD-L1:B7-1 interactions limit potentially pathogenic self-reactive effector T cell responses *in vivo*.

Discussion

PD-L1 has a key role in controlling the balance between T cell activation and tolerance. We recently identified B7-1 as a second binding partner for PD-L1, and showed that there are bidirectional interactions between B7-1 and PD-L1 that can inhibit T cell responses *in vitro* (16). In this study we have demonstrated that the B7-1:PD-L1 pathway plays a role in regulating T cell tolerance. We show that this pathway controls the responses of self-reactive T cells in the NOD mouse model of Type I diabetes.

The majority of approaches that have been used to analyze PD-L1 function to date cannot discriminate whether PD-L1 is exerting its inhibitory effects by binding to PD-1 or B7-1. We used the novel 10F.2H11 mAb, which we previously identified as a selective blocker of the PD-L1:B7-1 interaction (16) to analyze the function of this interaction *in vivo*. Here we further characterized 10F.2H11 mAb in cross blocking studies using two anti-PD-L1 mAb, 10F.9G2 and MIH5, both of which can block PD-L1:PD-1 and PD-L1:B7-1 interactions. 10F.2H11 and 10F.9G2 have similar bivalent affinities for PD-L1, but bind to distinct epitopes on PD-L1, while dual-blocker mAbs, MIH5 and 10F.9G2, have overlapping epitopes. We also determined that PD-L1 can functionally engage PD-1 when 10F.2H11 is bound to PD-L1. The co-crystal structure of PD-L1:PD-1 shows that PD-1 binds to the upper part of the GFCC′C″ face of the IgV domain of PD-L1 (29). While the co-crystal structure of PD-L1:B7-1 is not known, the surfaces of PD-L1 that were predicted by chemical cross-linking to bind to PD-1 and B7-1 partially overlapped, with the B7-1 binding surface being somewhat lower on the GFCC′C″ face of PD-L1(16). In PD-L2, the C″ and part of C′ have been deleted and if PD-L1 uses this region to bind to B7-1, this may explain why PD-L2 does not bind B7-1 (16, 29-31). Thus, it is plausible that the selective capability of 10F.2H11 to block the B7-1:PD-L1 interaction is due to its binding to PD-L1 in a region which is necessary for binding to B7-1, but not PD-1.

We compared the consequences of administering the 10F.2H11 and 10F.9G2 anti-PD-L1 mAbs to non-diabetic 6-7 or 13 week-old NOD mice to compare the effects of these anti-PD-L1 mAbs at early and late phases during the progression of diabetes. While we cannot rule out the possibility that differences in some property of these two rat IgG2b Abs *in vivo* (such as bioavailability) may lead to quantitative differences in their potencies, we have administered multiple doses at saturating concentrations (data not shown) to attempt to minimize these potential differences. We also evaluated potential effects of 10F.2H11 related to antibody-mediated deletion. Induction of diabetes by 10F.2H11 is unlikely to involve a depleting mechanism such as antibody-dependent cell-mediated cytotoxicity as we did not observe any increase in the numbers of cells undergoing cell death. The numbers of transferred T cells and recipient dendritic cells, both of which might be targets for deletion by virtue of their PD-L1 expression, were not decreased during the course of 8.3^+ T cell adoptive transfer experiments and in fact, we observed an increase in the number of transferred T cells in anti-PD-L1-treated mice (Supplemental Fig. 3). In addition, PD-L1 expressing cells were detected *ex vivo* from 10F.2H11-treated mice at similar levels to isotype control-treated mice using the MIH5 antibody (data not shown).

Although both anti-PD-L1 mAbs could lead to the onset of diabetes in NOD females, the timing of their effects was distinct. When given to either 6-7 or 13 week-old NOD mice, the 10F.9G2 mAb had profound effects, resulting in diabetes in 90% of the treated mice within 7 days. These findings are consistent with a previous study showing that blockade of PD-L1 (using MIH6, which we have found to be a dual blocker, unpublished observation) or PD-1 can accelerate the development of diabetes in NOD female mice (14). Notably, the 10F.2H11 mAb that blocks only the PD-L1:B7-1 interaction led to development of diabetes in 40% of the treated 6-7 week-old NOD mice over a 14-day period, but in 80% of 13-week-old NOD females within 7 days. The greater effect of 10F.2H11 treatment in older mice suggests that PD-L1:B7-1 interactions may be particularly important for regulating potentially pathogenic self-reactive effector T cells. To test this hypothesis, we used an adoptive transfer approach to compare the effects of 10F.2H11 or 10F.9G2 mAb administration to NOD SCID recipients of T cells from either prediabetic or diabetic NOD donors. Consistent with our findings in NOD mice, the 10F.2H11 mAb accelerated diabetes in NOD SCID recipients of T cells from diabetic, but not prediabetic, mice. These findings point to a critical role for the PD-L1:B7-1 pathway in inhibiting effector T cell functions *in vivo*.

In further adoptive transfer studies using BDC2.5 and 8.3 TCR transgenic T cells, we found that 10F.2H11 could accelerate responses of islet antigen-reactive $CD4^+$ and $CD8^+$ effector T cells. The BDC2.5 model is a very rapid and aggressive disease model, in which transferred T cells become rapidly activated *in vivo*. In the 8.3 model, T cells from diabetic donors, which already have an activated phenotype (data not shown) are transferred. Thus, the equal effect of 10F.2H11 and 10F.9G2 in accelerating or precipitating diabetes in these TCR transgenic models is consistent with a preferential role for PD-L1:B7-1 in controlling the functions of activated effector T cells.

We and others have found that PD-L1 can control peripheral T cell tolerance at multiple checkpoints. PD-L1 can inhibit activation and differentiation of naïve self-reactive T cells as well as expansion and functions of effector T cells. Our studies using the 10F.2H11 and 10F.9G2 mAb suggest that the PD-L1:B7-1 interaction primarily restrains self-reactive effector T cells, while PD-L1:PD-1 interactions predominate in controlling the initial activation of self-reactive T cells. It may be that the PD-L1:PD-1 pathway is a more potent inhibitory interaction, blockade of which is sufficient to break tolerance at all early phases of disease pathogenesis, while the PD-L1:B7-1 pathway has a more subtle role. Alternatively, the PD-

L1:PD-1 and PD-L1:B7-1 pathways may have overlapping or redundant functions at earlier phases, but unique or non-overlapping roles after initial T cell activation.

Further studies are needed to understand how the PD-L1:B7-1 pathway exerts its inhibitory functions *in vivo*. PD-1 and B7-1 are both expressed on activated T cells and PD-L1 expression is increased on T cells upon their activation. Expression of PD-L1 and B7-1 on activated T cells may explain the predominant function of the PD-L1:B7-1 pathway in controlling effector T cell responses. A recent study using a different “single-blocker” anti-PD-L1 Ab showed a role for the PD-L1:B7-1 pathway in a TCR transgenic model of T cell tolerance (32). This study invoked a role for B7-1 on T cells acting as an inhibitory receptor for PD-L1, but was unable to account for the majority of the effects of this antibody, which were independent of the expression of B7-1 on non-T cells and only partially dependent on B7-1 expression on T cells. Using the 8.3^+ T cell adoptive transfer model we analyzed the expression of both PD-1 and B7-1 on donor 8.3^+ T cells during the course of an adoptive transfer and found that B7-1 is in fact upregulated on donor T cells prior to PD-1. Since the affinity of the PD-L1:B7-1 interaction is lower than that of the PD-L1:PD-1 interaction (16), the existence of a sizeable population of $B7\text{-}1^+PD\text{-}1^-$ T cells may be an important target of PD-L1-mediated suppression via B7-1 and this population may in turn become the pathogenic population when the PD-L1:B7-1 interaction is blocked. Since both anti-PD-L1 antibodies used here block the PD-L1:B7-1 interaction, the fact that they have similar effects in this model may be explained by the possibility that the PD-L1:B7-1 interaction predominates in the first days after transfer, prior to upregulation of PD-1.

PD-1 and PD-L1 have become important therapeutic targets because of their key roles in pathogenesis of chronic viral infections, autoimmune diseases, tumor immunity, and transplantation tolerance. Blockade of PD-L1 can enhance T cell responses in the setting of chronic infection or cancer, whereas ligation of PD-L1 has the potential to suppress undesired T cell responses during autoimmunity or transplant rejection. Further work is needed to understand how to effectively manipulate PD-1 and PD-L1 to activate T cells in the setting of chronic infection or tumors, while minimizing the risk of autoimmunity and immunopathology. It may be that single- rather than dual-blockade will be preferable when modulating PD-L1 under some circumstances. Understanding whether PD-L1:PD-1 and PD-L1:B7-1 interactions have unique or overlapping roles in controlling T cell tolerance and immunopathology may provide insights for effective therapeutic strategies that target PD-L1 and PD-1.

Supplementary Material

Refer to Web version on PubMed Central for supplementary material.

Acknowledgments

We thank Mark Anderson for the gift of 8.3 NOD mice, Rod Bronson and the Dana-Farber Rodent Histopathology Core for assistance with histopathology, Sirisha Tatavarti, Kevin Allan, Flor Gonzalez and Robert Ortega for technical assistance, and Manish Butte for useful discussions.

This work was funded by the National Multiple Sclerosis Society grant FG 1805-A-1 (AMP) and the National Institute of Health grants PO1 AI56299 (AHS, MHS, BRB, GJF), R01 AI051559 (MHS, GJF), PO1 AI39671 (AHS), and R37 A1038310 (AHS).

References

1. Sheppard KA, Fitz LJ, Lee JM, Benander C, George JA, Wooters J, Qiu Y, Jussif JM, Carter LL, Wood CR, Chaudhary D. PD-1 inhibits T-cell receptor induced phosphorylation of the ZAP70/

CD3zeta signalosome and downstream signaling to PKCtheta. FEBS Lett. 2004; 574:37–41. [PubMed: 15358536]

2. Okazaki T, Maeda A, Nishimura H, Kurosaki T, Honjo T. PD-1 immunoreceptor inhibits B cell receptor-mediated signaling by recruiting src homology 2-domain-containing tyrosine phosphatase 2 to phosphotyrosine. Proc Natl Acad Sci U S A. 2001; 98:13866–13871. [PubMed: 11698646]
3. Keir ME, Butte MJ, Freeman GJ, Sharpe AH. PD-1 and its ligands in tolerance and immunity. Annu Rev Immunol. 2008; 26:677–704. [PubMed: 18173375]
4. Francisco LM, Sage PT, Sharpe AH. The PD-1 pathway in tolerance and autoimmunity. Immunol Rev. 236:219–242. [PubMed: 20636820]
5. Dong H, Zhu G, Tamada K, Chen L. B7-H1, a third member of the B7 family, co-stimulates T-cell proliferation and interleukin-10 secretion. Nat Med. 1999; 5:1365–1369. [PubMed: 10581077]
6. Freeman GJ, Long AJ, Iwai Y, Bourque K, Chernova T, Nishimura H, Fitz LJ, Malenkovich N, Okazaki T, Byrne MC, Horton HF, Fouser L, Carter L, Ling V, Bowman MR, Carreno BM, Collins M, Wood CR, Honjo T. Engagement of the PD-1 immunoinhibitory receptor by a novel B7 family member leads to negative regulation of lymphocyte activation. J Exp Med. 2000; 192:1027–1034. [PubMed: 11015443]
7. Latchman Y, Wood CR, Chernova T, Chaudhary D, Borde M, Chernova I, Iwai Y, Long AJ, Brown JA, Nunes R, Greenfield EA, Bourque K, Boussiotis VA, Carter LL, Carreno BM, Malenkovich N, Nishimura H, Okazaki T, Honjo T, Sharpe AH, Freeman GJ. PD-L2 is a second ligand for PD-1 and inhibits T cell activation. Nat Immunol. 2001; 2:261–268. [PubMed: 11224527]
8. Tseng SY, Otsuji M, Gorski K, Huang X, Slansky JE, Pai SI, Shalabi A, Shin T, Pardoll DM, Tsuchiya H. B7-DC, a new dendritic cell molecule with potent costimulatory properties for T cells. J Exp Med. 2001; 193:839–846. [PubMed: 11283156]
9. Brown KE, Freeman GJ, Wherry EJ, Sharpe AH. Role of PD-1 in regulating acute infections. Curr Opin Immunol.
10. Sharpe AH, Wherry EJ, Ahmed R, Freeman GJ. The function of programmed cell death 1 and its ligands in regulating autoimmunity and infection. Nat Immunol. 2007; 8:239–245. [PubMed: 17304234]
11. Zou W, Chen L. Inhibitory B7-family molecules in the tumour microenvironment. Nat Rev Immunol. 2008; 8:467–477. [PubMed: 18500231]
12. Yamazaki T, Akiba H, Iwai H, Matsuda H, Aoki M, Tanno Y, Shin T, Tsuchiya H, Pardoll DM, Okumura K, Azuma M, Yagita H. Expression of programmed death 1 ligands by murine T cells and APC. J Immunol. 2002; 169:5538–5545. [PubMed: 12421930]
13. Liang SC, Latchman YE, Buhlmann JE, Tomczak MF, Horwitz BH, Freeman GJ, Sharpe AH. Regulation of PD-1, PD-L1, and PD-L2 expression during normal and autoimmune responses. Eur J Immunol. 2003; 33:2706–2716. [PubMed: 14515254]
14. Ansari MJ, Salama AD, Chitnis T, Smith RN, Yagita H, Akiba H, Yamazaki T, Azuma M, Iwai H, Khoury SJ, Auchincloss H Jr, Sayegh MH. The programmed death-1 (PD-1) pathway regulates autoimmune diabetes in nonobese diabetic (NOD) mice. J Exp Med. 2003; 198:63–69. [PubMed: 12847137]
15. Keir ME, Liang SC, Guleria I, Latchman YE, Qipo A, Albacker LA, Koulmanda M, Freeman GJ, Sayegh MH, Sharpe AH. Tissue expression of PD-L1 mediates peripheral T cell tolerance. J Exp Med. 2006; 203:883–895. [PubMed: 16606670]
16. Butte MJ, Keir ME, Phamduy TB, Sharpe AH, Freeman GJ. Programmed death-1 ligand 1 interacts specifically with the B7-1 costimulatory molecule to inhibit T cell responses. Immunity. 2007; 27:111–122. [PubMed: 17629517]
17. Butte MJ, Pena-Cruz V, Kim MJ, Freeman GJ, Sharpe AH. Interaction of human PD-L1 and B7-1. Mol Immunol. 2008; 45:3567–3572. [PubMed: 18585785]
18. Ghiotto M, Gauthier L, Serriari N, Pastor S, Truneh A, Nunes JA, Olive D. PD-L1 and PD-L2 differ in their molecular mechanisms of interaction with PD-1. Int Immunol. 22:651–660. [PubMed: 20587542]
19. Latchman YE, Liang SC, Wu Y, Chernova T, Sobel RA, Klemm M, Kuchroo VK, Freeman GJ, Sharpe AH. PD-L1-deficient mice show that PD-L1 on T cells, antigen-presenting cells, and host

tissues negatively regulates T cells. Proc Natl Acad Sci U S A. 2004; 101:10691–10696. [PubMed: 15249675]

20. Keir ME, Freeman GJ, Sharpe AH. PD-1 regulates self-reactive CD8+ T cell responses to antigen in lymph nodes and tissues. J Immunol. 2007; 179:5064–5070. [PubMed: 17911591]
21. Wang J, Yoshida T, Nakaki F, Hiai H, Okazaki T, Honjo T. Establishment of NOD-Pdcd1-/- mice as an efficient animal model of type I diabetes. Proc Natl Acad Sci U S A. 2005; 102:11823–11828. [PubMed: 16087865]
22. Yadav D, Fine C, Azuma M, Sarvetnick N. B7-1 mediated costimulation regulates pancreatic autoimmunity. Mol Immunol. 2007; 44:2616–2624. [PubMed: 17289146]
23. Keir ME, Latchman YE, Freeman GJ, Sharpe AH. Programmed death-1 (PD-1):PD-ligand 1 interactions inhibit TCR-mediated positive selection of thymocytes. J Immunol. 2005; 175:7372–7379. [PubMed: 16301644]
24. Rodig N, Ryan T, Allen JA, Pang H, Grabie N, Chernova T, Greenfield EA, Liang SC, Sharpe AH, Lichtman AH, Freeman GJ. Endothelial expression of PD-L1 and PD-L2 down-regulates CD8+ T cell activation and cytolysis. Eur J Immunol. 2003; 33:3117–3126. [PubMed: 14579280]
25. Katz JD, Wang B, Haskins K, Benoist C, Mathis D. Following a diabetogenic T cell from genesis through pathogenesis. Cell. 1993; 74:1089–1100. [PubMed: 8402882]
26. Stadinski BD, Delong T, Reisdorph N, Reisdorph R, Powell RL, Armstrong M, Piganelli JD, Barbour G, Bradley B, Crawford F, Marrack P, Mahata SK, Kappler JW, Haskins K. Chromogranin A is an autoantigen in type 1 diabetes. Nat Immunol. 11:225–231. [PubMed: 20139986]
27. Herman AE, Freeman GJ, Mathis D, Benoist C. CD4+CD25+ T regulatory cells dependent on ICOS promote regulation of effector cells in the prediabetic lesion. J Exp Med. 2004; 199:1479–1489. [PubMed: 15184501]
28. Verdaguer J, Schmidt D, Amrani A, Anderson B, Averill N, Santamaria P. Spontaneous autoimmune diabetes in monoclonal T cell nonobese diabetic mice. J Exp Med. 1997; 186:1663–1676. [PubMed: 9362527]
29. Lin DY, Tanaka Y, Iwasaki M, Gittis AG, Su HP, Mikami B, Okazaki T, Honjo T, Minato N, Garboczi DN. The PD-1/PD-L1 complex resembles the antigen-binding Fv domains of antibodies and T cell receptors. Proc Natl Acad Sci U S A. 2008; 105:3011–3016. [PubMed: 18287011]
30. Lazar-Molnar E, Yan Q, Cao E, Ramagopal U, Nathenson SG, Almo SC. Crystal structure of the complex between programmed death-1 (PD-1) and its ligand PD-L2. Proc Natl Acad Sci U S A. 2008; 105:10483–10488. [PubMed: 18641123]
31. Freeman GJ. Structures of PD-1 with its ligands: sideways and dancing cheek to cheek. Proc Natl Acad Sci U S A. 2008; 105:10275–10276. [PubMed: 18650389]
32. Park JJ, Omiya R, Matsumura Y, Sakoda Y, Kuramasu A, Augustine MM, Yao S, Tsushima F, Narazaki H, Anand S, Liu Y, Strome SE, Chen L, Tamada K. B7-H1/CD80 interaction is required for the induction and maintenance of peripheral T cell tolerance. Blood.

Special abbreviations

PD-1	Programmed death-1
PD-L1	Programmed death-1 ligand 1
NOD SCID	NOD.CB17-Prkdc^{Scid}
8.3 NOD	NOD.Cg-Tg(TcraTcrbNY8.3)1Pesa/Dvs
PLN	pancreatic lymph node
7-AAD	7-amino-actinomycin D

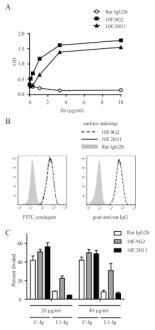

Figure 1. Anti-PD-L1 mAb 10F.2H11 does not interfere with functional PD-L1:PD-1 signaling, whereas 10F.9G2 does

A, Binding of 10F.9G2, 10F.2H11 and Rat IgG2b isotype control mAb to PD-L1-Ig fusion protein was compared by ELISA. *B*, Binding of 10F.9G2 or 10F.2H11 to PD-L1-transfected 300.19 cells assessed by flow cytometry. Directly conjugated mAb (left panel) or fluorescently conjugated anti-rat IgG secondary (right panel) were used. *C*, Functional engagement of PD-1 is inhibited by 10F.9G2, but not 10F.2H11. PD-1-overexpressing transgenic T cells were cultured on plates coated with anti-CD3 and either PD-L1-Ig fusion protein (L1-Ig) or control protein (C-Ig). After coating, plates were incubated with the indicated concentrations of anti-PD-L1 Abs or control Ab, washed and then T cells were added. Proliferation was measured by CFSE dilution of 7-AAD-negative T cells by flow cytometry. Data are representative of at least two independent experiments.

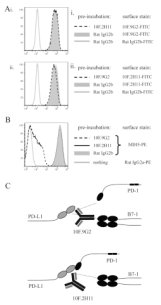

Figure 2. 10F.9G2 and 10F.2H11 recognize distinct epitopes of PD-L1

A, B. Analysis of epitopes recognized by 10F.9G2 and 10F.2H11 mAbs. PD-L1-transfected 300.19 cells were pre-incubated with 20 μg/ml purified antibody and then stained with fluorescently conjugated MIH5, 10F.9G2, 10F.2H11 or isotype control as indicated. *C*, Schematic depiction of the binding and blocking capabilities of the 10F.9G2 and 10F.2H11 mAbs. Data are representative of at least two independent experiments.

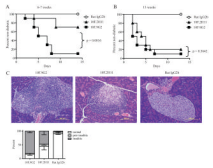

Figure 3. 10F.2H11 precipitates diabetes in NOD females in an age-dependent manner

6-7 week-old (*A*) or 13 week-old (*B*) NOD females were treated with 0.5 mg antibody i.p. on day 0, followed by 0.25 mg on days 2, 4, 6, 8 and 10 or until they became diabetic. n=10 for each group; data are representative of three independent experiments. *C*, 6-7 week old mice were treated on days 0 and 2 and pancreata were harvested on day 3. H&E stains of representative sections are shown. Left panel – 10F.9G2 (insulitis); middle panel – 10F. 2H11 (peri-insulitis with mild insulitis); right panel – Rat IgG2b isotype control (no insulitis). Scale bars in bottom right-hand corners represent 200 μm. Pancreata were scored as either normal (white) or as having peri-insulitis (light grey) or insulitis (dark grey).

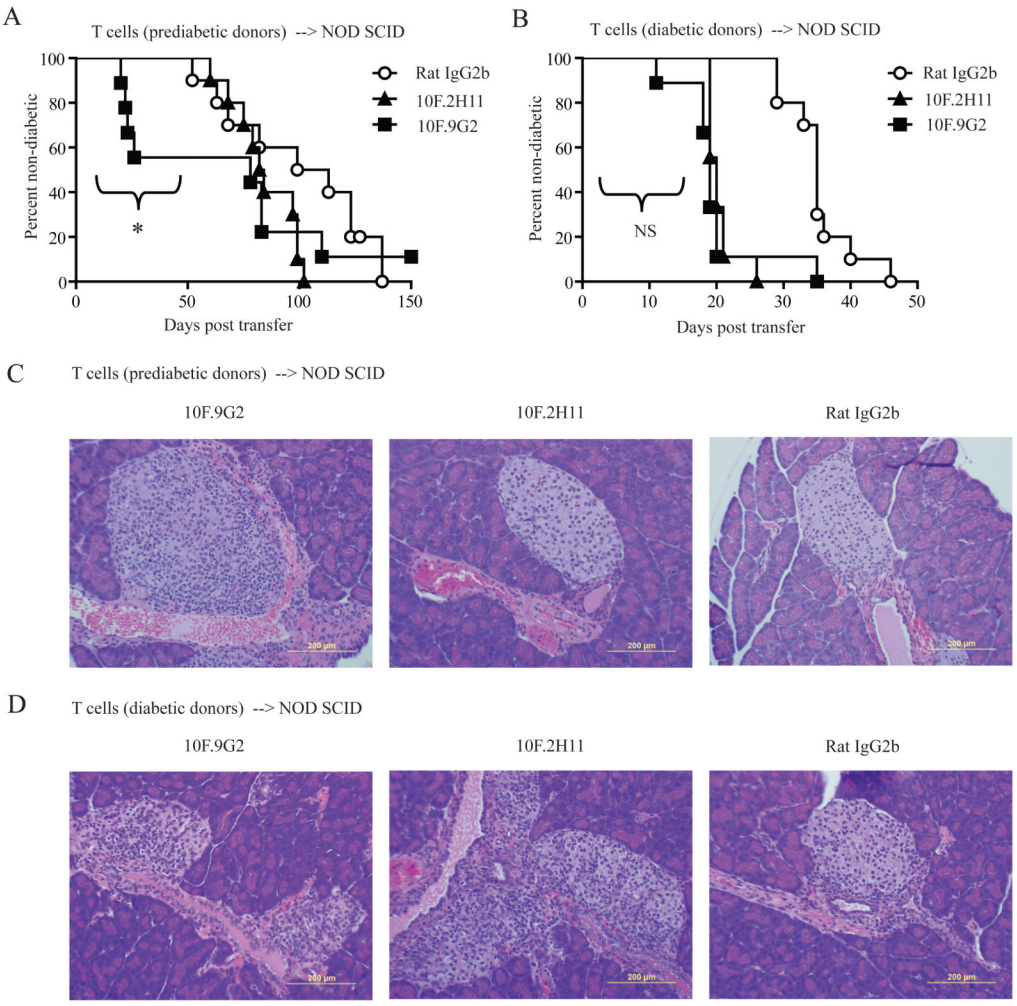

Figure 4. T cells from diabetic mice are more susceptible than T cells from prediabetic mice to the effects of 10F.2H11 antibody

$CD4^+$ and $CD8^+$ T cells from prediabetic (*A*) or diabetic (*B*) NOD females were transferred *i.v.* into NOD SCID recipients which were then treated with 0.5 mg antibody i.p. on day 0, followed by 0.25 mg on days 2, 4, 6, 8 and 10. *$p<0.05$ over the first 59 days for 10F.9G2 *vs.* 10F.2H11 treatment. For transfers from diabetic donors, the effects of 10F.9G2 *vs.* 10F.2H11 mAb administration were not significantly different over any time frame. Data are pooled from two independent experiments with similar results; n = at least 9 per group. Pancreata for histology were harvested 10 days after transfer of prediabetic (*C*) or diabetic (*D*) T cells. Left panels – 10F.9G2 (insulitis in C and D); middle panels – 10F.2H11 (no insulitis in C, insulitis in D); right panels – Rat IgG2b isotype control (no insulitis in C or D).

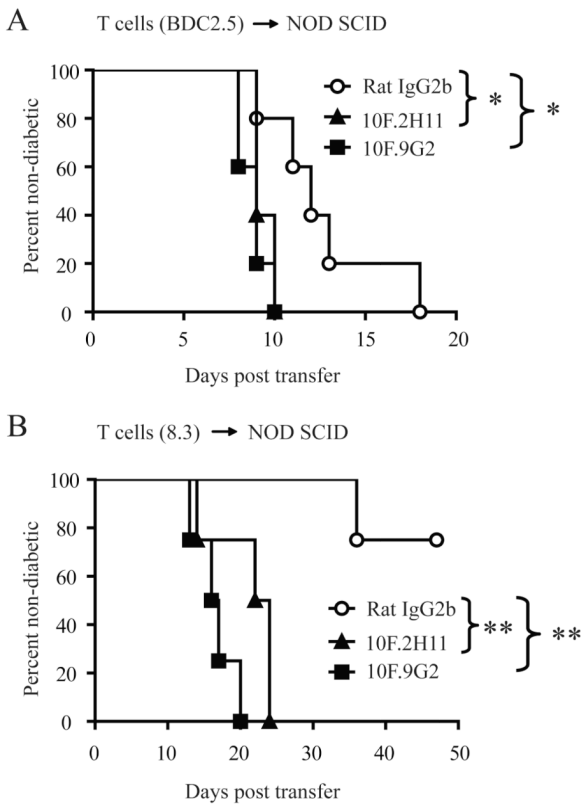

Figure 5. Both 10F.2H11 and 10F.9G2 antibodies precipitate diabetes transferred by islet antigen-specific transgenic CD4$^+$ or CD8$^+$ effector T cells

2×10^4 CD4$^+$Foxp3-GFP$^-$ T cells purified from BDC2.5 Foxp3-GFP NOD TCR transgenic mice (*A*) or 4.5×10^6 CD8$^+$ T cells purified from diabetic 8.3$^+$ NOD TCR transgenic mice (*B*) were transferred *i.v.* to NOD SCID recipients, which were then treated with 0.5 mg antibody i.p. on day 0, followed by 0.25 mg on days 2, 4, 6, 8 and 10. Data are representative of two and four experiments, respectively, each with at least four mice per group. *p<0.05; **p<0.005

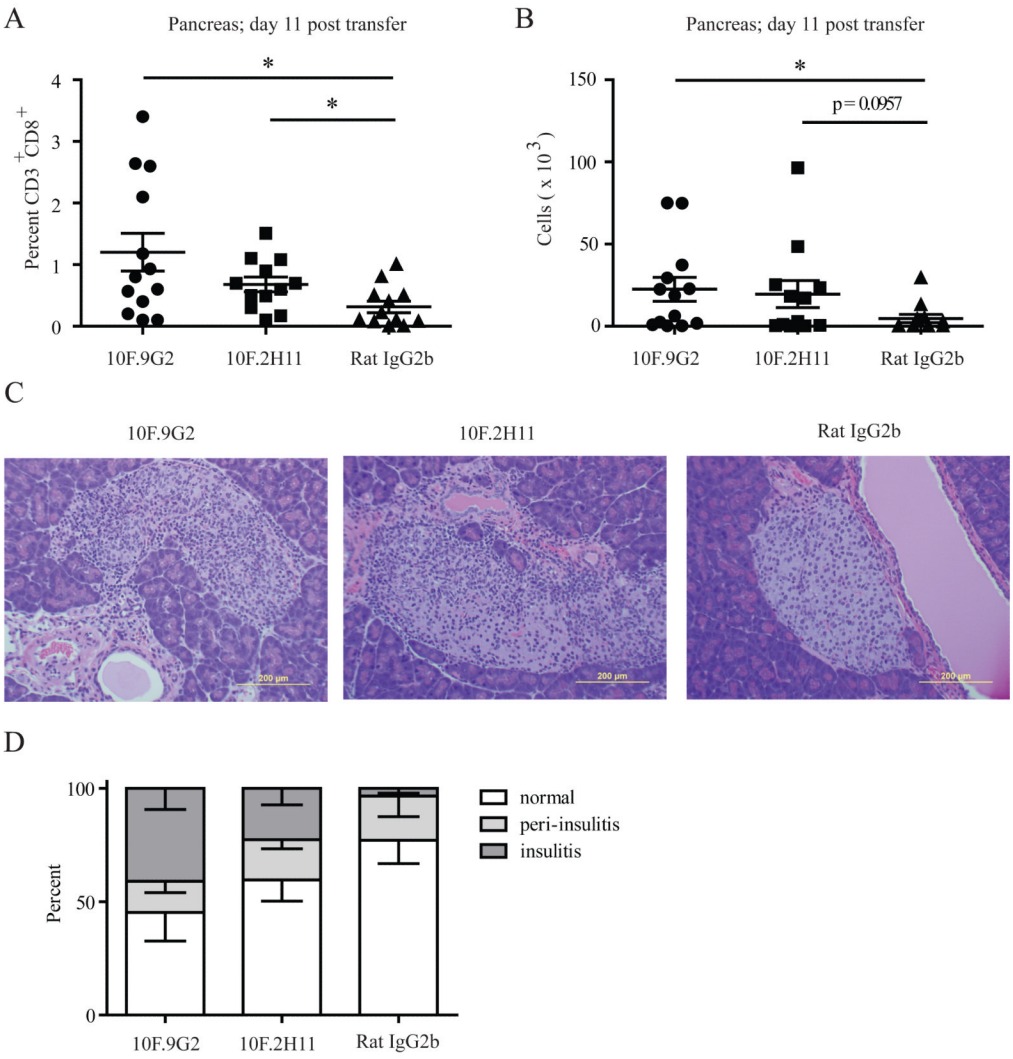

Figure 6. 10F.2H11 and 10F.9G2 mAb treatment increases islet infiltration by CD8$^+$ effector T cells

NOD SCID recipients of 8.3$^+$ NOD TCR transgenic T cells were treated with anti-PD-L1 antibodies or isotype control and analyzed on day 11 post transfer. Pancreatic infiltrates were analyzed for the percentage (*A*) and number (*B*) of CD3$^+$CD8$^+$ T cells. Pooled data from 3 independent experiments each with at least 3 mice per group are shown. *p<0.05. Pancreas sections showing islets were stained with H&E (*C*) and scored for insulitis (*D*). Left panel – 10F.9G2 (insulitis); middle panel – 10F.2H11 (insulitis); right panel – Rat IgG2b isotype control (no insulitis).

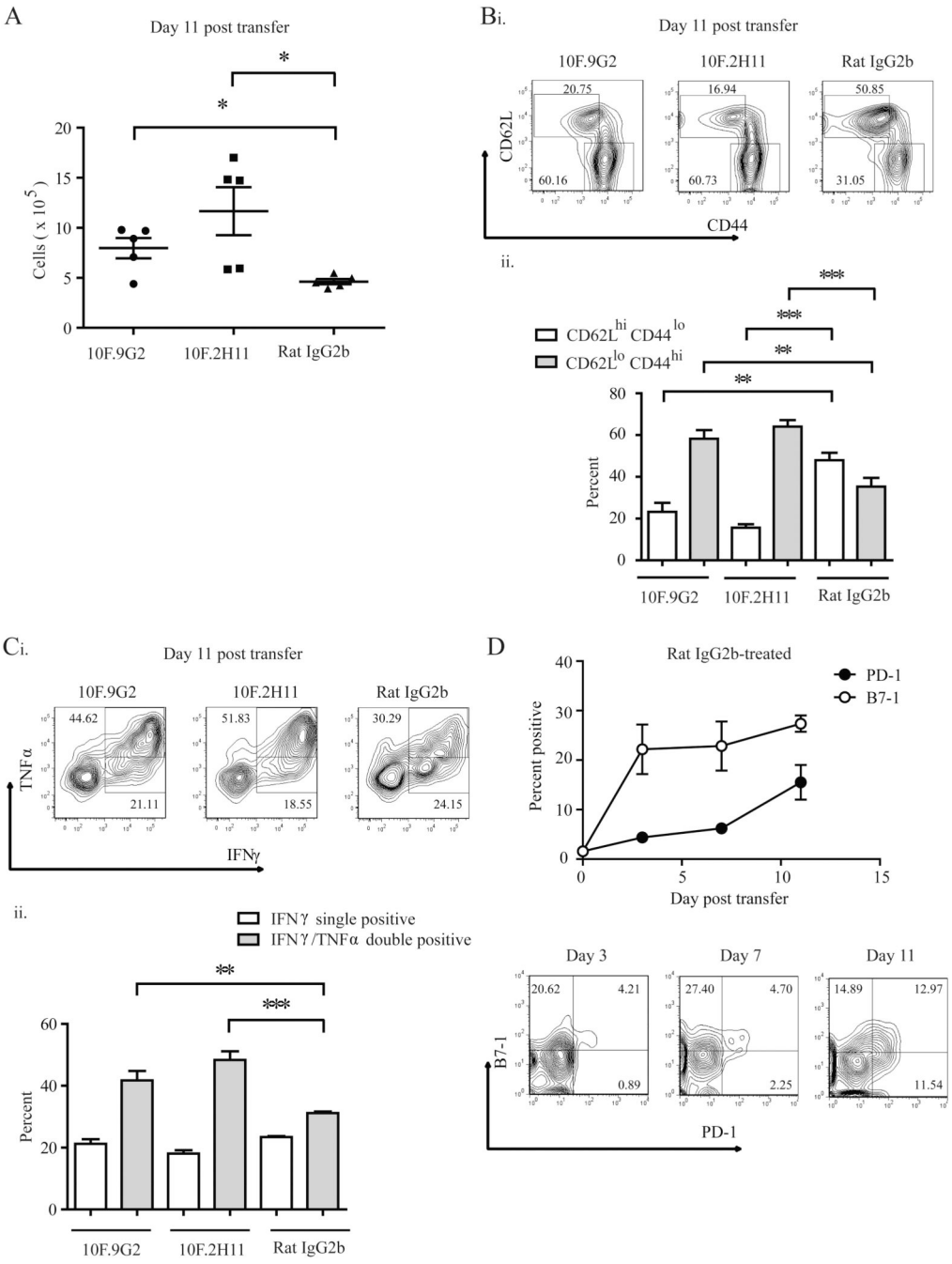

Figure 7. 10F.2H11 and 10F.9G2 mAbs increase CD8$^+$ effector T cell expansion, activation and cytokine production

NOD SCID recipients were given 8.3$^+$ NOD TCR transgenic T cells, treated with anti-PD-L1 antibodies or isotype control, and analyzed on the indicated day post transfer. Splenic CD3$^+$CD8$^+$ T cells were evaluated by flow cytometry for numbers (*A*), activation (*B*), cytokine production (*C*) and B7-1 and PD-1 expression (*D*). For *B* and *C*, representative flow cytometry plots (*i*) and cumulative data (*ii*) are shown. (*A*-*C*) shows data representative of three independent experiments, each with five mice per group; (*D*) shows representative FACS plots and pooled data from two independent experiments **p<0.005; ***p<0.0005